

**Random spin freezing in  $Ce_2MIn_8$  ( $M=Co,Rh,Ir$ ) heavy-fermion materials**G. D. Morris, R. H. Heffner, N. O. Moreno, P. G. Pagliuso, J. L. Sarrao, and S. R. Dunsiger  
*Los Alamos National Laboratory, K764, Los Alamos, New Mexico 87545, USA*G. J. Nieuwenhuys  
*Kamerlingh Onnes Laboratory, Leiden University, Postbus 9504, 2300 RA Leiden, The Netherlands*D. E. MacLaughlin  
*Department of Physics, University of California, Riverside, California 92521, USA*O. O. Bernal  
*Physics Department, California State University, Los Angeles, California 90032, USA*  
(Received 21 October 2003; revised manuscript received 25 February 2004; published 18 June 2004)

Previous specific heat and resistivity measurements have established a preliminary phase diagram for the evolution of magnetic order in heavy-fermion materials  $Ce_2M_xIr_{1-x}In_8$ ,  $M=Co, Rh$ ; a possible quantum critical point (QCP) was postulated for  $Ce_2IrIn_8$ . Zero-field muon spin relaxation studies in  $Ce_2RhIn_8$  find very rapidly damped oscillations below the Néel temperature  $T_N=2.8$  K, indicating a broad field distribution consistent with the presence of an incommensurate magnetic structure. In  $Ce_2IrIn_8$ , and in samples in which several percent of Ir is substituted by Co or Rh, muon spin relaxation spectra reveal the onset of a Lorentzian field distribution, with zero mean, characteristic of disordered spin freezing. The onset temperature for this freezing depends on composition; it is smallest, but still nonzero, in  $Ce_2IrIn_8$ , ruling out a QCP. The evolution of magnetism in the temperature-composition phase diagram indicates that the type of magnetic ordering depends systematically on the degree of Ce- $M$  hybridization and the local Ce environment.

DOI: 10.1103/PhysRevB.69.214415

PACS number(s): 75.20.Hr, 71.27.+a, 76.75.+i

**I. INTRODUCTION**

Materials in the  $Ce_nMIn_{3n+2}$  series of heavy-fermion compounds have demonstrated a wide range of magnetic and unconventional superconducting behavior.<sup>1</sup> Of particular interest has been the temperature-doping phase diagrams<sup>2</sup> showing overlapping magnetic and superconducting regions for  $n=1$  and  $M=Co, Rh$ , and Ir. Here, recent muon spin relaxation ( $\mu$ SR) (Ref. 3) and other experiments<sup>4</sup> in  $CeRh_{0.5}Ir_{0.5}In_5$  have demonstrated microscopic coexistence of magnetic and superconducting order. Also of considerable importance are temperature-pressure phase diagrams and measurements of the thermal conductivity and microwave impedance in  $CeCoIn_5$ , for example, which show similarities to the generic cuprate superconductors.<sup>5-7</sup> Underlying the physics of these unconventional superconducting systems is the role of possible quantum critical behavior<sup>8</sup> in shaping the materials' properties.

The  $Ce_nMIn_{3n+2}$  materials form tetragonal structures which may be viewed as  $n$  layers of  $CeIn_3$  sandwiched between layers of  $MIn_2$ . This is illustrated in Fig. 1. The cubic parent material  $CeIn_3$  has antiferromagnetic (AFM) order below  $T_N=10$  K with a Ce moment of  $0.48-0.65\mu_B$ .<sup>9</sup> Below  $T_N=3.8$  K  $CeRhIn_5$  has an incommensurate antiferromagnetic structure in which Ce moments with magnitude  $0.75(2)\mu_B$  spiral  $107^\circ$  per unit cell along the  $c$  axis with ordering vector  $(1/2, 1/2, 0.297)$ .<sup>10</sup> Both  $CeIn_3$  (Ref. 11) and  $CeRhIn_5$  (Ref. 5) become superconducting with the application of pressure, which destroys the AFM state. This has given rise to the hypothesis that superconductivity in these systems occurs near an AFM quantum critical point (QCP).

After extensive research on the single-layer  $n=1$  compounds, recent attention has turned to examining the physics of the  $n=2$  materials. Transport, susceptibility and thermodynamic measurements of the  $M=Co, Ir$  and  $Rh$   $n=2$  compounds have established a preliminary phase diagram for the evolution of magnetism across temperature-composition space.<sup>12</sup> This is shown in Fig. 2, where one sees that the signature of a magnetic transition at  $T=T_m$  has a minimum for  $Ce_2IrIn_8$  and a maximum for  $Ce_2RhIn_8$ . The magnetic structure of the Ce moments in  $Ce_2RhIn_8$  was first determined to be commensurate AFM,<sup>13</sup> but subsequent neutron

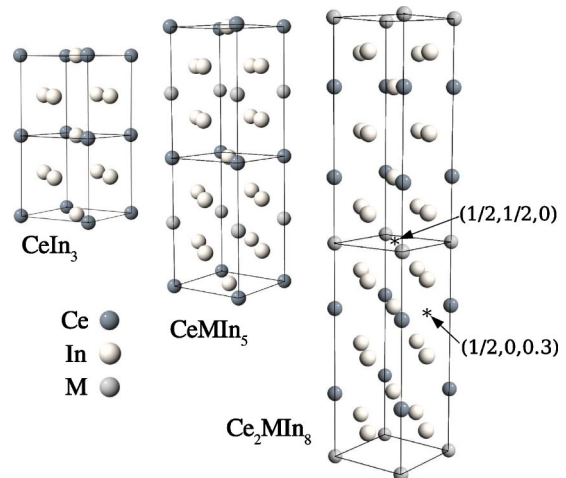


FIG. 1. Structures of  $CeIn_3$ ,  $CeMIn_5$ , and  $Ce_2MIn_8$ . Two possible muon sites in  $Ce_2MIn_8$  are indicated by the arrows.

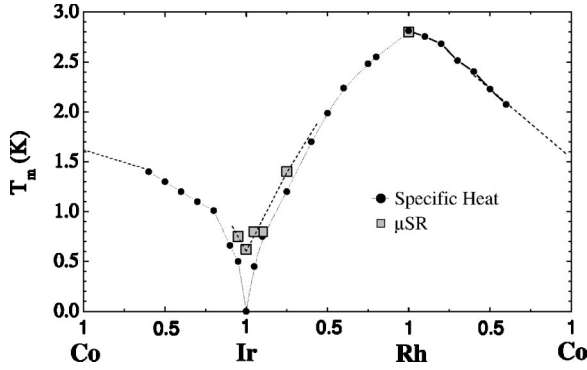


FIG. 2. Temperature-composition phase diagram of magnetic transition temperature  $T_m$  in  $\text{Ce}_2\text{Ir}_{1-x}\text{M}_x\text{In}_8$ ,  $M=\text{Co}$ , Ir, Rh from specific heat data (dots) (Ref. 12) and zero-field  $\mu\text{SR}$  data (squares).

diffraction experiments have identified magnetic peaks associated with both commensurate and incommensurate ordering.<sup>14</sup> The temperature dependence of the specific heat<sup>12</sup> shows progressively smaller and broader peaks as  $T_m$  approaches zero, hinting at the existence of a possible quantum critical point at the  $M=\text{Ir}$  composition.

We have performed  $\mu\text{SR}$  experiments on several compositions of  $\text{Ce}_2\text{Ir}_{1-x}\text{M}_x\text{In}_8$ ,  $M=\text{Co}$ , Ir, and Rh, to investigate the evolution of magnetic order in these systems and, in particular, to search for possible small electronic magnetic moments near the  $M=\text{Ir}$  composition. Absence of magnetic order would be consistent with a true QCP. The  $\mu\text{SR}$  technique<sup>15</sup> is particularly suitable for such an investigation, having a sensitivity high enough to detect an ordered moment as small as  $0.001\mu_B$ .

## II. EXPERIMENTAL TECHNIQUE

All samples were single crystals grown at Los Alamos from stoichiometric mixtures of Ce and Ir, Rh, or Co in an In flux. Single crystals grown this way form flat plates with the  $c$  axis normal to the crystal face.<sup>16</sup>

Conventional time-differential  $\mu\text{SR}$  experiments were carried out with the GPS and LTF spectrometers at the Paul Scherrer Institute, Switzerland, and the M15 and M20 channels at TRIUMF in Vancouver, Canada. The  $\mu\text{SR}$  technique involves the implantation of fully spin-polarized positive muons which are trapped at interstitial sites. The time dependence of the muon spin polarization is monitored through the anisotropic distribution of positrons produced in the parity-violating weak decay of the muons. In general the magnetic moment of each muon has a component transverse to the local field  $\mathbf{B}$  and a longitudinal component parallel to  $\mathbf{B}$ . Each muon's magnetic moment precesses about  $\mathbf{B}$  at a frequency  $\omega_\mu = \gamma_\mu B = 2\pi \times 135.54 \text{ MHz}/T \times B$ , and the damping rate of the transverse component of spin polarization is proportional to the rms width of the local field distribution. The relaxation rate of the longitudinal spin polarization is proportional to the spectral weight of transverse fluctuations of  $\mathbf{B}$  at the muon Larmor frequency  $\omega_\mu$ .<sup>18</sup>

## III. EXPERIMENTAL RESULTS

### A. $\text{Ce}_2\text{RhIn}_8$

$\text{Ce}_2\text{RhIn}_8$  exhibits AFM order at  $T_N=2.8 \text{ K}$ ; the magnetic structure of this material, as well as the field-temperature

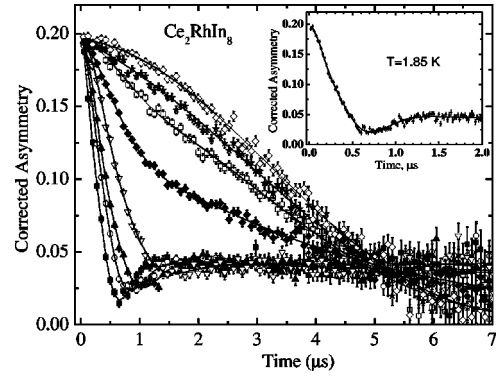


FIG. 3. Zero field muon spin polarization signals in  $\text{Ce}_2\text{RhIn}_8$  at temperatures (from top to bottom)  $T=4, 3, 2.8, 2.7, 2.6, 2.4, 2.2$ , and  $1.65 \text{ K}$ . The solid lines are fits as described in the text. Inset: Close examination of the first  $0.5 \mu\text{s}$  of data reveals two very rapidly damped oscillating components.

phase diagram,<sup>17</sup> is still under investigation. We collected zero-field  $\mu\text{SR}$  spectra on  $\text{Ce}_2\text{RhIn}_8$  at temperatures from  $1.65\text{--}4.0 \text{ K}$  in the GPS spectrometer on a single crystal flat plate measuring about  $8 \times 8 \times 0.5 \text{ mm}$ , with the  $c$  axis along the beam and the  $a$  axis vertical. The muon spin was in the  $ac$  plane, about  $50^\circ$  from the  $c$  axis. Spectra shown in Fig. 3 were collected with positron detectors for up-down muon decay asymmetries. Low-temperature data ( $0.022\text{--}1.1 \text{ K}$ ) were acquired in the LTF on a mosaic of several crystals, each with its  $c$  axis normal to the crystal faces, but not oriented in the  $ab$  plane. Muons in the LTF were implanted with their spins parallel to the  $c$  axis and longitudinal relaxation spectra were recorded with backward-forward counters.

At  $T=4.0 \text{ K}$  the muon spin relaxation function is described by a Gaussian Kubo-Toyabe  $G_{\text{KT}}(t) = \frac{1}{3} + \frac{2}{3}(1$

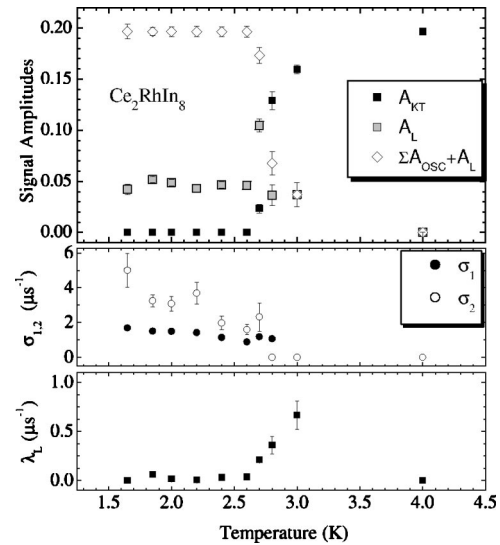


FIG. 4. Temperature dependence of the total magnetic amplitude  $\sum_i (A_{\text{osc}})_i + A_L$ , the magnetic relaxing amplitude  $A_L$ , the nuclear Kubo-Toyabe amplitude  $A_{\text{KT}}$ , the inhomogeneous relaxation rates  $\sigma_1$  and  $\sigma_2$ , and the magnetic spin lattice relaxation rate  $\lambda_L$  in  $\text{Ce}_2\text{RhIn}_8$  from fitting the zero field  $\mu\text{SR}$  spectra to  $G_z = A_{\text{KT}}G_{\text{KT}}(t) + G_m(t)$ , where  $G_m(t)$  is given by Eq. (1).

$-\Delta_n^2 t^2) \exp(-\Delta_n^2 t^2/2)$ , where  $\Delta_n/\gamma_\mu = 0.25$  mT is characteristic of In nuclear dipolar fields.<sup>19</sup> On cooling highly damped oscillations become evident below  $T_N$  (Fig. 3). A longitudinal field of 20 mT resulted in a complete decoupling from the internal field (see Fig. 7 for  $\text{Ce}_2\text{IrIn}_8$ ), indicating<sup>19</sup> a broad field distribution resulting from electronic moments which are static on time scales of microseconds. A broad distribution of fields is also consistent with an incommensurate magnetically ordered structure between about 1.5 K and  $T_N$ .<sup>14</sup>

Our choice of fitting function below  $T_N$  is guided by several issues. First,  $\text{Ce}_2\text{RhIn}_8$  is known to possess incommensurate AFM order between  $T_N = 2.8$  and 1.6 K. Below 1.6 K an additional commensurate component also develops.<sup>14</sup> Magnetic order generally results in finite average fields at muon sites, unlike random magnetic moments which produce a field distribution centered on zero. We know from high transverse-field spectra (not reported here) that muons occupy two sites in these materials, as in the  $n=1$  compounds.<sup>20</sup> Although not yet determined, likely sites include the  $(1/2, 1/2, 0)$  site [in analogy with the dominant  $(1/2, 1/2, 1/2)$  site in the  $n=1$  materials<sup>20</sup>] and the  $(1/2, 0, \sim 0.3)$  site between Ce atoms, as shown in Fig. 1. A trace of two oscillations is seen in the first  $\mu\text{s}$  of the asymmetry plot shown in the inset to Fig. 3. The lower frequency component, strongly damped, results in the minimum at  $t=0.7$   $\mu\text{s}$ . The higher frequency component produces an inflection point in the asymmetry at  $t=0.2$   $\mu\text{s}$ . The spectra are very similar to those observed in  $\text{CeRh}_{0.5}\text{Ir}_{0.5}\text{In}_5$  below 2 K,<sup>3</sup> where two lines in zero field with frequencies differing by a factor of about 3 are more clearly evident. Because the oscillating signals in  $\text{Ce}_2\text{RhIn}_8$  are rapidly relaxed, it is not possible to fit the asymmetry with two free frequency parameters at all temperatures. We found that fitting with a fixed frequency ratio was feasible, however, and that a 1:3 ratio gave a good fit at all temperatures, as in  $\text{CeRh}_{0.5}\text{Ir}_{0.5}\text{In}_5$ . We have thus fit the data in the ordered phase to  $G_z(t) = G_m(t)$ , where

$$G_m(t) = \sum_i (A_{\text{osc}})_i \cos(\omega_{\mu i} t + \phi) \exp(-\sigma_i^2 t^2) + A_L \exp(-\lambda t), \quad (1)$$

where  $i=1, 2$ . In the crossover region just below  $T_N$ , where both nuclear dipolar and magnetically ordered signals were observed, the relaxation was fit to  $G_z(t) = A_{\text{KT}} G_{\text{KT}}(t, \Delta_n) + G_m(t)$ . The total asymmetry was measured well above  $T_N$  in weak transverse field and held fixed in fitting all the zero-field runs. Also, the parameter  $\Delta_n$  was held fixed at lower temperatures.

Figure 4 shows the temperature dependence of the fractions  $A_L$ ,  $\sum_i (A_{\text{osc}})_i$ , and  $A_{\text{KT}}$ , and the rates  $\sigma_1$ ,  $\sigma_2$ , and  $\lambda$ . The transition is rather sharp. The temperature dependence of the lower frequency is shown in Fig. 5. Note that there appears to be a break in the trend of the frequency data between 1.1 and 1.7 K. This is qualitatively consistent with neutron diffraction experiments<sup>14</sup> which show a different magnetic structure for  $T$  above and below 1.6 K.

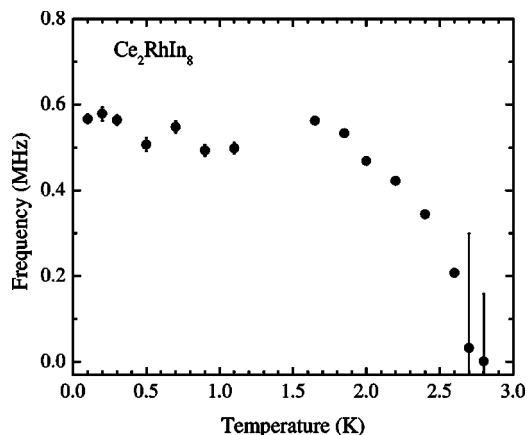


FIG. 5. Temperature dependence of the muon precession frequency in  $\text{Ce}_2\text{RhIn}_8$ .

### B. $\text{Ce}_2\text{Ir}_{1-x}\text{M}_x\text{In}_8$

Zero field spectra were collected with the TRIUMF M15 dilution refrigerator with the  $c$  axis parallel to the muon beam momentum and initial muon spin direction. Representative longitudinal spin relaxation spectra, from positron detectors for backward-forward asymmetry, recorded in  $\text{Ce}_2\text{IrIn}_8$  are shown in Fig. 6.

Samples with 5% Co or 5, 10, and 25% Rh substituted for Ir displayed qualitatively similar relaxation functions and temperature dependencies. At temperatures  $\geq 1$  K in  $\text{Ce}_2\text{IrIn}_8$  the relaxation function follows a Gaussian Kubo-Toyabe form characteristic of nuclear dipolar fields. On cooling, an additional magnetic relaxation mechanism is apparent. No coherent precession signal—as seen in  $\text{Ce}_2\text{RhIn}_8$  and indicative of a nonzero average field from ordered magnetism—was found in any of these samples. Application of longitudinal fields showed that these magnetic signals completely decouple between 20–40 mT for the pure Ir- and

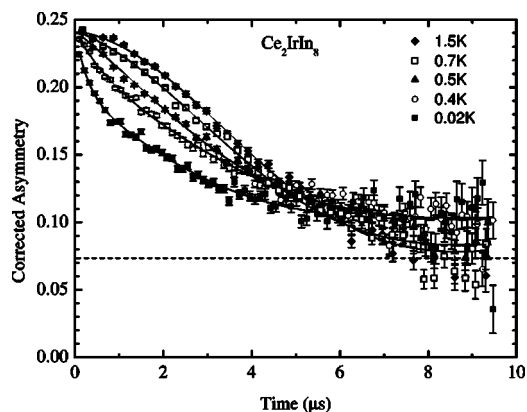


FIG. 6. Temperature dependence of the zero field muon spin relaxation spectra in  $\text{Ce}_2\text{IrIn}_8$ . As the temperature is lowered the spectra change from the Gaussian Kubo-Toyabe form, characteristic of nuclear dipolar broadening, to two-exponential relaxation (corresponding to two muon sites), indicating magnetic freezing with a broad distribution of local fields. The dashed line indicates the non-relaxing background fraction arising from muons stopping in refrigerator parts.

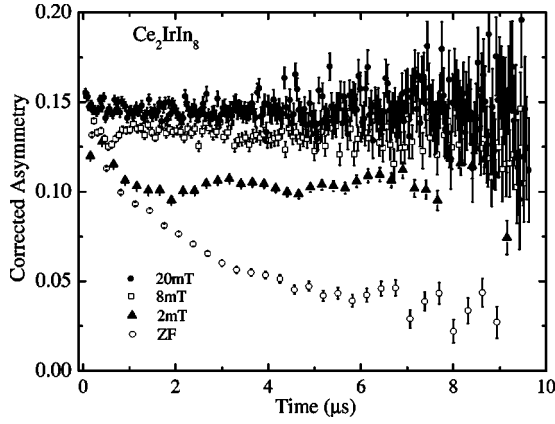


FIG. 7. Longitudinal  $\mu$ SR spectra in  $\text{Ce}_2\text{IrIn}_8$  at 0.02 K for fields of 0, 2, 8, and 20 mT applied parallel to the muon spin. A nonrelaxing component partly from muons stopping in silver refrigerator parts is subtracted from the spectra shown.

Co/Rh-doped samples (see Fig. 7). Here, “decoupling” refers to the loss of relaxation when the applied field is significantly larger than the local static field distribution. Relaxation from fluctuating fields does not generally vanish in a longitudinal field unless the muon Larmor frequency is at least comparable to the characteristic fluctuation rate. Thus, the observed magnetic relaxation is from a static (on a time scale of  $\mu\text{s}$ ) distribution of local fields.<sup>19</sup>

At low temperatures the spectra are very well described by the product of  $G_{\text{KT}}(t, \Delta_n)$  times the sum of two exponentials  $G_m(t)$  given by

$$G_m(t) = A_1 \exp(-\lambda_1 t) + A_2 \exp(-\lambda_2 t), \quad (2)$$

plus a nonrelaxing signal due both to muons stopping in silver parts of the dilution refrigerator (this background fraction is indicated by the horizontal dashed line) and a longitudinal component of the muon spin which is parallel to the local static magnetic field. Although there is clearly a nonre-

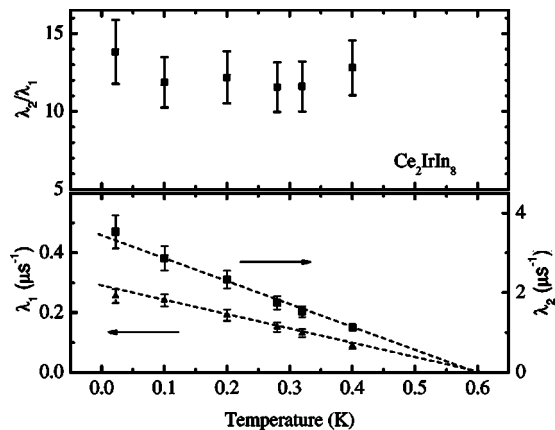


FIG. 8. Temperature dependence of the zero-field relaxation rates  $\lambda_1$  and  $\lambda_2$  in  $\text{Ce}_2\text{IrIn}_8$  obtained by fitting the magnetic relaxation to Eq. (2), as described in the text. Above about 0.4 K the two rates are too small to resolve. Both relaxation rates extrapolate to zero at about 0.6 K and their ratio is constant.

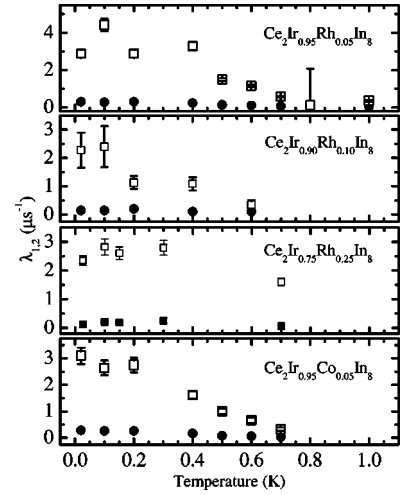


FIG. 9. Temperature dependence of the zero-field relaxation rates  $\lambda_1$  and  $\lambda_2$  in  $\text{Ce}_2(\text{Ir}, M)\text{In}_8$ ,  $M = \text{Rh}, \text{Co}$ , obtained by fitting the magnetic relaxation to Eq. (2), as described in the text.

laxing longitudinal component, the spectra do not determine if the polarization function eventually recovers at long times to 1/3 of the initial amplitude, which would be indicative of an isotropic local field distribution, or whether the polarization remains small at long times indicating static fields predominantly in the  $a$ - $b$  plane. The value of  $\Delta_n$  was again determined from high temperature data and held fixed at low temperatures.

Figure 8 shows the temperature dependencies of  $\lambda_1$  and  $\lambda_2$  in  $\text{Ce}_2\text{IrIn}_8$ , together with their ratio. One immediately sees that the ratio is independent of temperature, and that the temperature dependencies of  $\lambda_1$  and  $\lambda_2$  also extrapolate to the same onset temperature. Also, the ratio  $A_1/A_2$  was kept temperature independent in fitting. We interpret this to mean that the two relaxation components correspond to the two muon sites, which see the same field distribution, but with hyperfine fields differing by about a factor of 12. The larger rate  $\lambda_2 \cong 4 \mu\text{s}^{-1}$  (whose signal has an amplitude of about 1/3 of the total) corresponds to a local field width  $\Delta B$  of about 6 mT, completely consistent with a decoupling field of between 20–40 mT  $\cong 5 \times \Delta B$ .<sup>19</sup> The Co/Rh-doped samples show very similar results, i.e., the magnetic relaxation is well described by the sum of two exponentials, and all the spectra exhibit decoupling in fields  $\cong 20$ –40 mT. Data for the doped samples is shown in Fig. 9.

Table I shows the rough onset temperature  $T_m$  for the observed magnetic relaxation, as well as the low-temperature

TABLE I. Extrapolated onset temperatures of magnetic relaxation and low  $T$  linewidths in  $\text{Ce}_2\text{IrIn}_8$  and (Co, Rh)-doped samples.

Sample	$T_m, \text{K}$	$\lambda_2(T \rightarrow 0), \mu\text{s}^{-1}$
$\text{Ce}_2\text{IrIn}_8$	0.6	3.6(4)
$\text{Ce}_2\text{Ir}_{0.95}\text{Co}_{0.05}\text{In}_8$	0.75	2.9(3)
$\text{Ce}_2\text{Ir}_{0.95}\text{Rh}_{0.05}\text{In}_8$	0.8	3.5(5)
$\text{Ce}_2\text{Ir}_{0.90}\text{Rh}_{0.10}\text{In}_8$	$\sim 0.8$	2.3(6)
$\text{Ce}_2\text{Ir}_{0.75}\text{Rh}_{0.25}\text{In}_8$	$\sim 1.4$	2.4(2)

exponential linewidth for the larger of the two rates  $\lambda_2$ . One sees that the onset temperatures roughly follow the trend of the specific heat data in Fig. 2, although clearly the onset temperature of the  $\mu$ SR rate in  $Ce_2IrIn_8$  is not zero.

In  $Ce_2RhIn_8$  below  $T_N$ , where long-range order is present, the frequencies and linewidths of the two oscillating signals differ by the same factor of approximately 3. It is not surprising that a Lorentzian distribution of local fields from disordered moments in  $Ce_2IrIn_8$  results in a different ratio (12:1) in relaxation rates.

#### IV. DISCUSSION

The purpose of this study was to investigate the magnetic properties of the  $Ce_2MIn_8$  phase diagram ( $M=Ir, Co,$  and  $Rh$ ), particularly in the region where specific heat and susceptibility show a minimum in the magnetic ordering temperature near  $M=Ir$ , indicating a possible QCP. We find a well-defined signature of magnetic order corresponding to a finite, static local field in  $Ce_2RhIn_8$ . There is also an indication of a change in magnetic structure between 1.1 and 1.7 K, the latter in qualitative agreement with recent neutron diffraction experiments.<sup>14</sup> In all of the other materials we find no coherent precession of the muon spin and, hence, no magnetic order with a finite local field at the muon sites. Instead, we observe a freezing of the local magnetic field characterized by a static, exponential relaxation function, implying a Lorentzian local-field distribution, with zero mean, similar to that seen in spin glasses.<sup>21</sup> The line shape is not identical to the characteristic isotropic spin-glass function,<sup>21</sup> however, which contains an initial exponential relaxation followed by a dip and a return to one third of the initial asymmetry at long times. Here the relaxation is just a simple exponential.

An exponential muon spin relaxation results from a local field distribution which is broad compared to the mean magnitude. Usually, such a distribution results from the presence of a low concentration of randomly distributed moments so that most muons, far from these moments, would see nearly zero field, while the few muons close to the moments would sense a high field. For the dilute Co- or Rh-doped systems one could imagine local magnetic clusters of Co- or Rh-rich regions having relatively large Ce moments (because  $Ce_2RhIn_8$ , for example, is magnetically ordered) with the rest of the volume containing small or zero Ce moments. We crudely estimate the concentration of randomly dispersed full Ce moments ( $J=5/2$ ) necessary to produce the measured Lorentzian linewidth ( $\approx 0.5-5.0 \mu s^{-1}$ ) to be about 0.1–1.0% of the available Ce sites.<sup>22</sup>

An alternative scenario could in principle be dense Ce moments with a broad distribution of moment sizes. In this case, the observed field spreads for the two muon sites of  $\Delta B \approx 0.6-6.0$  mT correspond to an average Ce moment of  $\approx 0.002-0.02 \mu_B$ , assuming dipolar  $Ce-\mu^+$  coupling for the muon at the  $(\frac{1}{2}, \frac{1}{2}, 0)$  site, for example. For  $Ce_2IrIn_8$ , whose counterpart in the single-layer  $CeIrIn_5$  is nonmagnetic (and thus inclusions of this material yield no magnetic islands), the necessary field distributions could possibly be accounted for by defects, vacancies and strain, which might yield a

distribution of moment sizes through nonuniform Ce-Ir hybridization (see discussion below).

We emphasize that the finding of spin freezing in  $Ce_2IrIn_8$  is particularly important because, if the magnetism is intrinsic, then a QCP is definitively ruled out. Even if the source of the magnetic freezing observed here is extrinsic (e.g., due to defects/strain) this could easily cause the non-Fermi-liquid behavior observed in transport<sup>23</sup> in this material, thus masquerading as a signature of a QCP. In this regard it is worth noting that the residual resistivity  $\rho_0$  in  $Ce_2IrIn_8$  ( $\approx 25 \mu\Omega$  cm) is much larger than in  $CeIrIn_5$  (a few  $\mu\Omega$  cm) and is at least  $50\times$  greater than in  $La_2IrIn_8$ . This large  $\rho_0$  could likely be caused by the spin freezing observed here.

Finally, we wish to point out a correlation in the  $Ce_nMIn_{3n+2}$  class of materials which could shed some light on this investigation. First note that apparently the degree of hybridization in the  $n=1$  compounds between the Ce and  $d$ -spin atoms increases as one goes from Rh to Ir to Co. Thus,  $CeRhIn_5$  is an AFM, while  $CeIrIn_5$  and  $CeCoIn_5$  are superconductors with critical temperatures of 0.4 and 2.2 K, respectively. It has also been noted that this progression in hybridization follows the trend of an increasing  $c$ -axis/ $a$ -axis ratio.<sup>1</sup> Furthermore, there is a clear structural progression in the series of materials, namely, that along the  $c$  axis each Ce atom in  $CeIn_3$  has two nearest-neighbor (NN) Ce atoms, while in  $CeIrIn_5$  each Ce atom has two NN Ir atoms and in  $Ce_2IrIn_8$  each Ce atom has one NN Ce and one NN Ir atom. This progression could be interpreted to correlate well with the existence of long-range AFM in  $CeIn_3$ , no spin ordering in  $CeIrIn_5$  and random-spin freezing in  $Ce_2IrIn_8$ . (Note also that in  $Ce_2RhIn_8$  the degree of hybridization is sufficiently small that long-range AFM can exist in this structure.) In the dense-moment hypothesis described above for  $Ce_2IrIn_8$  the small-moment spin freezing might be due to Ce-Ce interactions between only partially delocalized Ce moments, in a structural setting where each Ce atom has on average both a Ce and an Ir NN along the  $c$  axis, but a NN Ce in the  $a$ - $b$  plane. Defects or atomic-site interchange could introduce the necessary randomness, and strain could change the  $c$ -axis/ $a$ -axis ratio in parts of the sample allowing small magnetic moments to develop. The presence of a small second phase with a slightly different  $c$ -axis/ $a$ -axis ratio has apparently been identified<sup>24</sup> as the likely cause of the zero-resistance anomaly<sup>1</sup> above the bulk superconducting transition temperature in  $CeIrIn_5$ . Thus, these systems appear to be interesting ones in which the relative degrees of localization/itinerancy in Ce systems can be systematically investigated by changing the local Ce environment.

#### ACKNOWLEDGMENTS

This work was supported in part by U.S. NSF Grants No. DMR-0102293 (UC Riverside) and DMR-0203524 (CSU Los Angeles). Work at Los Alamos was performed under the auspices of the U.S. Department of Energy. We would like to acknowledge helpful discussions with Dr. Z. Fisk, Dr. Mike Hundley, Dr. D. Pines, and Dr. J. D. Thompson.

- <sup>1</sup>C. Petrovic, R. Movshovich, M. Jaime, P. G. Pagliuso, M. F. Hundley, J. L. Sarrao, Z. Fisk, and J. D. Thompson, *Europhys. Lett.* **53**, 354 (2001); C. Petrovic, P. G. Pagliuso, M. F. Hundley, R. Movshovich, J. L. Sarrao, J. D. Thompson, and Z. Fisk, *J. Phys.: Condens. Matter* **13**, L337 (2001); R. Movshovich, M. Jaime, J. D. Thompson, C. Petrovic, Z. Fisk, P. G. Pagliuso, and J. L. Sarrao, *Phys. Rev. Lett.* **86** 5152 (2001).
- <sup>2</sup>P. G. Pagliuso, C. Petrovic, R. Movshovich, D. Hall, M. F. Hundley, J. L. Sarrao, J. D. Thompson, and Z. Fisk, *Phys. Rev. B* **64**, 100503(R) (2001); P. G. Pagliuso, R. Movshovich, A. D. Bianchi, N. Nicklas, N. O. Moreno, J. D. Thompson, M. F. Hundley, J. L. Sarrao, and Z. Fisk, cond-mat/0107266 (unpublished).
- <sup>3</sup>G. D. Morris, R. H. Heffner, J. E. Sonier, D. E. MacLaughlin, O. O. Bernal, G. J. Nieuwenhuys, A. T. Savici, P. G. Pagliuso, and J. L. Sarrao, *Physica B* **326**, 390 (2003); cond-mat/0301309 (unpublished).
- <sup>4</sup>T. Mito, S. Kawasaki, Y. Kawasaki, G.-q. Zheng, Y. Kitaoka, D. Aoki, Y. Haga, and Y. Ōnuki, *Phys. Rev. Lett.* **90**, 077004 (2003); G.-q. Zheng, N. Yamaguchi, K. Tanabe, Y. Kitaoka, J. L. Sarrao, and J. D. Thompson (unpublished).
- <sup>5</sup>H. Hegger, C. Petrovic, E. G. Moshopoulou, M. F. Hundley, J. L. Sarrao, Z. Fisk, and J. D. Thompson, *Phys. Rev. Lett.* **84**, 4986 (2000).
- <sup>6</sup>K. Izawa, H. Yamaguchi, Y. Matsuda, H. Shishido, R. Settai, and Y. Ōnuki, *Phys. Rev. Lett.* **87**, 057002 (2001).
- <sup>7</sup>Rodrigo J. Ormeno, A. Sibley, Colin E. Gough, S. Sebastian, and I. R. Fisher, *Phys. Rev. Lett.* **88**, 047005 (2002).
- <sup>8</sup>S. Sachdev, *Quantum Phase Transitions* (Cambridge University Press, Cambridge, 1999).
- <sup>9</sup>A. Beniot, J. X. Boucherle, P. Convert, J. Flouquet, J. Palleau, and J. Schweizer, *Solid State Commun.* **34**, 293 (1980); J. M. Lawrence and S. M. Shapiro, *Phys. Rev. B* **22**, 4379 (1980).
- <sup>10</sup>W. Bao, P. G. Pagliuso, J. L. Sarrao, J. D. Thompson, Z. Fisk, J. W. Lynn, and R. W. Erwin, *Phys. Rev. B* **62**, R14 621 (2000); **63**, 219901(E) (2001); **67**, 099903(E) (2003).
- <sup>11</sup>I. R. Walker, F. M. Grosche, D. M. Freye, and G. G. Lonzarich, *Physica C* **282**, 303 (1997).
- <sup>12</sup>N. O. Moreno, M. F. Hundley, P. G. Pagliuso, R. Movshovich, M. Nicklas, J. D. Thompson, J. L. Sarrao, and Z. Fisk, *Physica B* **312-313**, 274 (2002).
- <sup>13</sup>W. Bao, P. G. Pagliuso, J. L. Sarrao, J. D. Thompson, Z. Fisk, and J. W. Lynn, *Phys. Rev. B* **64**, 020401(R) (2001).
- <sup>14</sup>A. Llobet (private communication).
- <sup>15</sup>J. H. Brewer, in *Encyclopedia of Applied Physics*, edited by G. L. Trig (VCH Publishers, New York, 1994), Vol. 11, p. 23; A. Schenck, *Muon Spin Rotation Spectroscopy: Principles and Applications in Solid State Physics* (Hilger, Bristol, Boston, 1985).
- <sup>16</sup>R. T. Macaluso, J. L. Sarrao, N. O. Moreno, P. G. Pagliuso, J. D. Thompson, F. R. Fronczek, M. F. Hundley, A. Malinowski, and J. Y. Chan, *Chem. Mater.* **15**, 1394 (2003).
- <sup>17</sup>A. L. Cornelius, P. G. Pagliuso, M. F. Hundley, and J. L. Sarrao, *Phys. Rev. B* **64**, 144411 (2001).
- <sup>18</sup>T. McMullen and E. Zaremba, *Phys. Rev. B* **18**, 3026 (1978).
- <sup>19</sup>R. S. Hayano, Y. J. Uemura, J. Imazato, N. Nishida, T. Yamazaki, and R. Kubo, *Phys. Rev. B* **20**, 850 (1979).
- <sup>20</sup>A. Schenck, D. Andreica, F. N. Gygax, D. Aoki, and Y. Ōnuki, *Phys. Rev. B* **66**, 144404 (2002).
- <sup>21</sup>Y. J. Uemura, T. Yamazaki, D. R. Harshman, M. Senba, and E. J. Ansaldo, *Phys. Rev. B* **31**, 546 (1985).
- <sup>22</sup>G. A. Gist and S. A. Dodds, *Phys. Rev. B* **30**, 2340 (1984), and references therein.
- <sup>23</sup>J. S. Kim, N. O. Moreno, J. L. Sarrao, J. D. Thompson, and G. R. Stewart, *Phys. Rev. B* (to be published).
- <sup>24</sup>E. G. Moshopoulou (unpublished).